31st Congress of the International Council of the Aeronautical Sciences

Belo Horizonte, Brazil; September 09-14, 2018

RESOLVENT-BASED CONTROL OF STREAKS IN BOUNDARY LAYERS

Petrônio A. S. Nogueira* , **André V. G. Cavalieri*** , **Ardeshir Hanifi**** , **Dan S. Henningson****
***Instituto Tecnológico de Aeronáutica, São José dos Campos, SP, 12228-900, Brazil , ****Dept. of Mechanics, Linné FLOW Centre, SeRC, KTH Royal Institute of Technology, SE-100 44 Stockholm, Sweden**

Keywords: *control, turbulence, transition*

Abstract

In the present work, we investigate efficient placement of sensors and actuators for closed-loop control of boundary-layer flows. The focus of this work is on the transitional flow cases where perturbation field is dominated by streaks. This is done using a reduced-order model based on resolvent analysis, an approach that also allows us to analyse the sensitivity of the flow response to control. A numerical sensitivity analysis was performed in this first approach, leading to conclusions about best choices of velocity components to be sensed and directions to be forced. Afterwards, we compared the performance between gaussian and shear sensors at the wall, focusing on the damping of the first resolvent gain using these devices. We close the work with the analysis of a plasma actuator, a configuration closer to standard choices for this kind of problem in both simulations and experiments.

1 Introduction

The presence of streamwise elongated structures in the near wall region of wall-bounded flows has been detected since the 70's. These structures, called streaks, are regions where the streamwise velocity of the flow alternates between values higher and lower than the spanwise average, and are governed by linear growth mechanisms as described by [1]. Streaks were found to be relevant for flow stability analysis, and shown to be responsible for subcritical transition to turbulence in some cases, such as transition of boundary layers subject to significant free-stream turbulence [2]. Streaks are also present in fully turbulent flows, showing their robustness and importance as a fundamental part of the flow dynamics, as shown in [3, 4].

In parallel with this, many efforts were made to delay transition to turbulence in boundary layers, which could reduce substantially the friction drag of wings. Many strategies have been tested in the last few years, but one of the main obstacles for applying them in aircraft is sensor and actuator placement, including the question of how many sensors and actuators are necessary to delay transition [5, 6]. Efficient choices of sensors and actuators is crucial to obtain energy savings by closed-loop control [7].

This is one of the main challenges of new concepts for control in boundary layers. The linear quadratic Gaussian (LQG) strategy allows optimal control for a given sensor/actuator configuration [8], but new setups would represent a new system with different matrices, which requires a new optimization for each case. Therefore, it is not obvious to determine efficient positions for sensors and actuators, and this is the objective of this work. For that, we will analyse this problem using resolvent analysis, focusing on boundary-layer transition by elongated streaks, as in [9], now with the inclusion of a proportional control.

The paper is organised as follows: first, we present the closed-loop resolvent operator as a

function of the control matrix $\mathbf{K}_c$; this formulation allows us to evaluate the effect of different actuator and sensor shapes in the optimal resolvent gain, which can be interpreted as a measure of the efficiency of the control regarding the most responsive structures in the flow. Afterwards, we present the shapes of sensors and actuators chosen for the study, followed by the results for each configuration. A discrete numerical sensitivity of the gains is performed by including small control amplitudes and narrow Gaussian sensors and actuators, which turned out to be an important tool to analyse the results of more complex configurations, such as plasma actuators and shear sensors.

2 Mathematical Model

We follow here the same formulation from [10], now for a Blasius boundary layer taken as a base flow. From the linearised Navier-Stokes and continuity equations, we can obtain the linear system, in operator notation,

$$\mathrm{i}\omega\boldsymbol{\psi} = \mathbf{A}\boldsymbol{\psi} + \mathbf{B}f, \tag{1}$$

where all variables are Fourier transformed in time, axial and spanwise directions (t, x and z transformed to frequency ω and wavenumbers k_x and k_z, respectively), so $\boldsymbol{\psi} = \boldsymbol{\psi}(k_x, y, k_z, \omega)$, with y being the wall-normal coordinate, and the form of the matrices can be seen in Appendix A. In this formulation, f is a tridimensional body force and $\boldsymbol{\psi} = [v\ \eta]^T$, where v and η are wall normal velocity and vorticity, respectively. Writing the system in terms of the velocity components, we have:

$$\boldsymbol{\phi} = \mathbf{C}\boldsymbol{\psi} \tag{2}$$

where $\boldsymbol{\phi} = [u\ v\ w]^T$ denotes the three components of velocity fluctuations in Cartesian coordinates. If the $\mathbf{A}$ operator is stable, from equations (1) and (2), we can write a transfer function relating forcing f to response $\boldsymbol{\phi}$,

$$\boldsymbol{\phi} = \left[\mathbf{C}\left(\mathrm{i}\omega - \mathbf{A}\right)^{-1}\mathbf{B}\right] f \Rightarrow \boldsymbol{\phi} = \mathbf{R}f \tag{3}$$

With the system written as equation (3), we can perform a singular value decomposition such that $\mathbf{R} = \mathbf{U}\Sigma\mathbf{V}^H$, where the columns of $\mathbf{U}$ form an orthogonal basis of response modes and the lines of $\mathbf{V}^H$ form an orthogonal basis of forcing modes, with these matrices linked by gains σ_i in the diagonal matrix Σ. Thus, the analysis can be used to project every disturbance and response in the $(\mathbf{U}, \Sigma, \mathbf{V})$ space, meaning that the forcing and response related to the maximum gain σ_i will be the most relevant ones in the domain.

The inclusion of active control in this problem is made by including a term $\mathbf{B}_c f_c$ in the right hand side of equation (1). The control strategy used in this first analysis is proportional, leading to $f_c = \mathbf{K}_c\boldsymbol{\phi}$. This leads to a closed-loop resolvent given by

$$\boldsymbol{\phi} = \left[\mathbf{C}\left(\mathrm{i}\omega\mathbf{I} - \mathbf{A} - \mathbf{B}_c\mathbf{K}_c\mathbf{C}\right)^{-1}\mathbf{B}\right] f \Rightarrow \boldsymbol{\phi} = \mathbf{R}_c f \tag{4}$$

We perform the resolvent analysis with the modified system shown in equation (4). The matrix $\mathbf{K}_c$ is used to link the sensing components (u, v or w) with the actuation directions x, y and z such that:

$$\begin{bmatrix} f_{c_x} \\ f_{c_y} \\ f_{c_z} \end{bmatrix} = \begin{bmatrix} K_{xu} & K_{xv} & K_{xw} \\ K_{yu} & K_{yv} & K_{yw} \\ K_{zu} & K_{zv} & K_{zw} \end{bmatrix} \begin{bmatrix} u \\ v \\ w \end{bmatrix}. \tag{5}$$

Each component of this matrix is a submatrix that selects the region that will be sensed and where the forcing will act.

For this analysis, we chose $k_x = \omega = 0$, $k_z = 1.5$ and $Re = 1000$ as a representative case, focusing on control of streaks. The base-flow is taken as the Blasius boundary layer, normalised by the displacement thickness δ^*.

3 Choices of Sensor and Actuators

The formulation as written in equation (4) gives us freedom to choose any shape of sensors and actuators for the problem. The ones chosen for the present study are defined in the following sections.

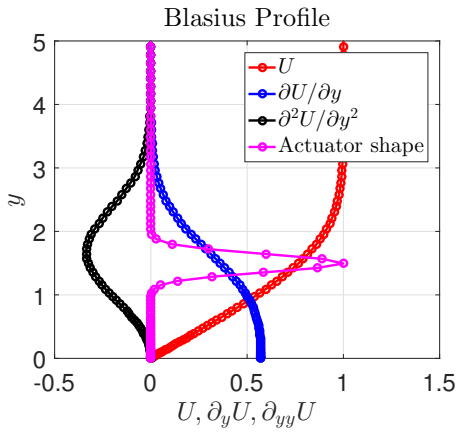

Fig. 1 Boundary layer profile, the derivatives and the actuator shape.

3.1 Gaussian Sensor and Gaussian Actuator

Firstly, we start with a Gaussian shape for both sensor and actuator, such that each component of the control matrix takes the form:

$$K_{xu} = A_c e^{-(\frac{y_m - y_s}{L_s})^2} e^{-(\frac{y_n - y_a}{L_a})^2} \tag{6}$$

where A_c is the control gain, y_m, y_n are the spatial coordinates related respectively to the sensor and actuator, y_s, y_a are the center of sensing and actuation and L_s, L_a are Gaussian widths. This approach is useful to explore the sensitivity of the resolvent gains with the wall-normal position of the actuator/sensor, providing information about the spatial support of efficient sensors and actuators. The variation of the gain with these positions will be closer to a continuous sensitivity analysis for pointwise sensors and actuators if the Gaussian width is small, in comparison with δ^*, and if the amplitude of the forcing is close to infinitesimal. Thus, we set $L_s = L_a = 0.2$ and $|A_c| = 10^{-4}$ in this analysis. The profile shape, its derivatives and the actuation shape can be seen in Figure 1.

3.2 Shear Sensor and Gaussian Actuator

Going one step closer to a real application, we chose a different kind of sensor: now, instead of sensing one velocity component for the feedback, we will sense the shear stress $\partial u/\partial y$ at the wall ($y = 0$) and perform the same analysis made for the previous case. For this case, the axial component of the forcing term, for instance, can be written as:

$$\begin{bmatrix} f_{c_{x_{y=0}}} \\ \dots \\ f_{c_{x_{y=H}}} \end{bmatrix} = [\mathcal{A}][\mathcal{S}] \begin{bmatrix} u_{y=0} \\ \dots \\ u_{y=H} \end{bmatrix} \tag{7}$$

where $[\mathcal{A}]$ defines the actuation shape and $[\mathcal{S}]$ is related to what is sensed inside the flow. For this case, we set $[\mathcal{S}] = D$, where D is the wall-normal derivation matrix and

$$[\mathcal{A}] = A_c e^{-(\frac{y_n - y_a}{L_a})^2}. \tag{8}$$

Since the actuator is kept exactly the same as in the previous approach, this analysis confirms and summarises the trends identified using the previous combination of sensors and actuators. More importantly, the comparison between this case and the previous one will show if sensing shear would lead to a better efficiency.

3.3 Shear Sensor and Plasma Actuator

The previous formulation was further developed in order to consider an actuator with a different shape, even closer to real applications. In this particular case, we chose to use the same actuator shape used by [11] (which is now considered in the matrix $[\mathcal{A}]$), with sensors for shear stress at the wall. In this analysis, we chose to vary a stretching parameter h, which changes the peak of atuation and also increases the region of influence of the actuator, as can be seen in Figure 2. The magnitude of actuation was kept constant in $|A_c| = 10^{-4}$.

Following the same strategy of the previous analysis, our focus was to evaluate the influence of the variation of the stretching parameter h in the gains σ from the resolvent analysis, differing from the previous study mainly by the length of actuation; now the actuator is considered to be at the wall, with different regions of influence. Even though plasma actuators are mounted on the wall, they generate a corresponding body force with some support inside the flow [12], and we here

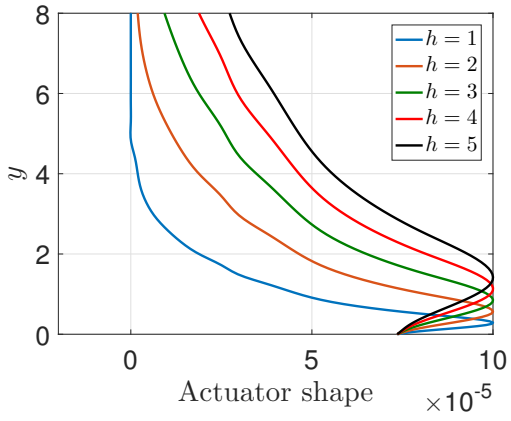

Fig. 2 Shape of actuation for several values of stretching factor h.

evaluate how such support may affect control efficiency.

4 Results

With the configurations defined, we proceed to the evaluation of optimal forcing and responses for the closed-loop resolvent operator. In each calculation, we investigate the reduction of the maximum resolvent gain (σ_1) compared with the uncontrolled case (σ_0), which will give an idea of the efficency of each control strategy.

4.1 Gaussian Sensor and Gaussian Actuator

For the first case, we varied the position of the center of actuation and sensing, exploring the influence of the spatial support of sensors and actuators in the resolvent gains for the controlled problem. This simulation were made isolating the influence of each component of the control matrix; doing that, we could also evaluate which components of velocity are more efficient for sensing and which directions of forcing would lead to higher reductions in the gains. These results can be seen in Figures 3 - 5, where $\Delta\sigma = \sigma_1 - \sigma_0$.

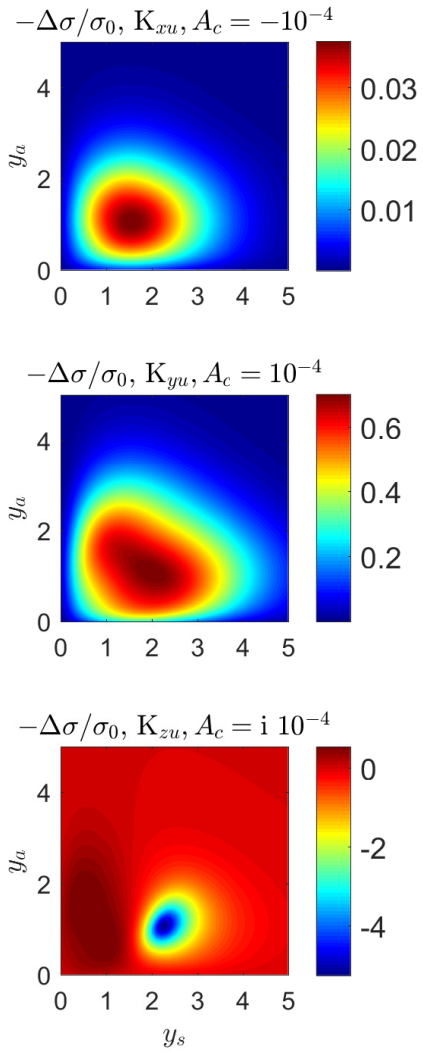

Fig. 3 Sensitivity of the first resolvent gain with change of actuator and sensor position. Sensor placed for streamwise velocity and actuation in each cartesian direction.

There are two main characteristics that stand out from Figures 3 - 5. The first one comes from the levels of reduction/increase in each contour plot: looking at Figures 4 and 5 one can see that the variation of the gains are rather small, except when the control forcing is in the same direction as the velocity component sensed (components K_{yv}, K_{zw} of the control matrix); in other words, the components $K_{xv}, K_{xw}, K_{yw}, K_{zv}$ do not affect the magnitude of the gains substantially. On the

other hand, the opposite trend happens when the streamwise velocity component is sensed: although the K_{xu} is related to variation with amplitudes comparable with the K_{yv}, K_{zw} components, the other ones shown in Figure 3 have much higher amplitudes than any other combination of actuator and sensor, meaning that sensing streamwise velocity is more efficient than sensing any other velocity component, and acting in the wall-normal/spanwise direction should also lead to higher reduction of gains by closed-loop control.

The second characteristic is related to the positon where the sensor and actuators work better. In all plots of Figures 3 - 5 a "hot spot" can be identified, a well defined region of the sensing/acting space where one could obtain higher reductions of the gains. For example, this region is located around $y_a = 1$ and $y_s = 2$ for the component K_{yu}, varying slightly for the other components. From that, one can conclude that, in order to design efficient actuator/sensor combinations, it would be better if the spatial support of these devices reach those positions.

This result is closely related to the underlying physics of the problem. For the chosen wavenumbers, the Blasius boundary layer is dominated by the lift-up phenomenon [1, 3], with optimal forcing shaping as streamwise vortices, which generates streaks as optimal response. Consequently, in order to mitigate this phenomenon, one should act to damp these vortices, or in other words, the actuation should be in the wall-normal/spanwise directions. Moreover, since the most responsive structure in the flow is a streak leading to fluctuations in streamwise velocity, the velocity component that will have higher amplitudes in the flow will be u; that explains why sensing this component is more efficient than sensing any other.

The regions for efficient sensing and acting are also related to optimal forcing and responses coming from the open-loop resolvent analysis. Figure 6 shows velocity and forcing components for both controlled and uncontrolled cases using K_{yu}, $y_a = 1.5$ and $y_s = 0.5$. As can be seen for the uncontrolled case, both optimal forcing

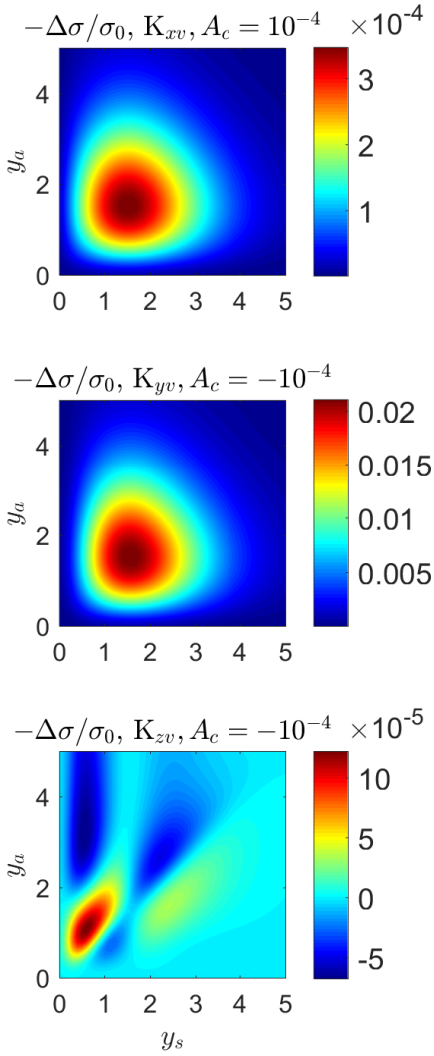

Fig. 4 Sensitivity of the first resolvent gain with change of actuator and sensor position. Sensor placed for wall-normal velocity and actuation in each cartesian direction.

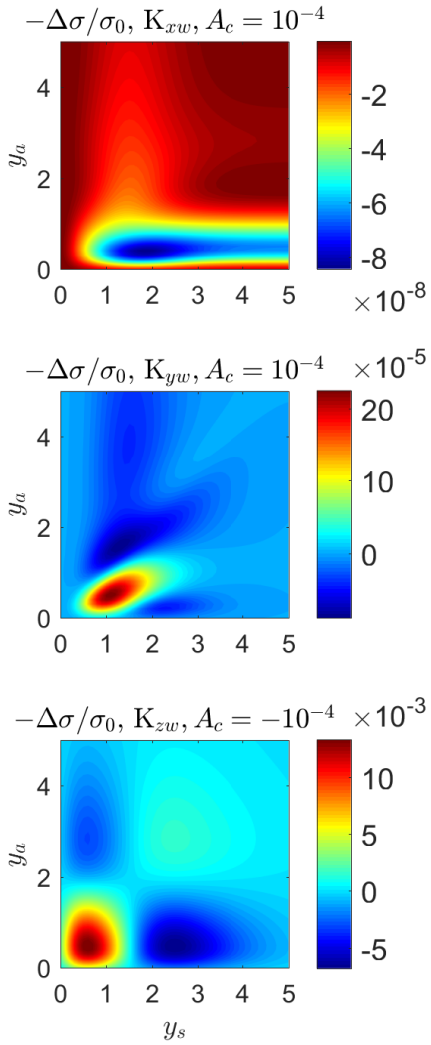

Fig. 5 Sensitivity of the first resolvent gain with change of actuator and sensor position. Sensor placed for spanwise velocity and actuation in each cartesian direction.

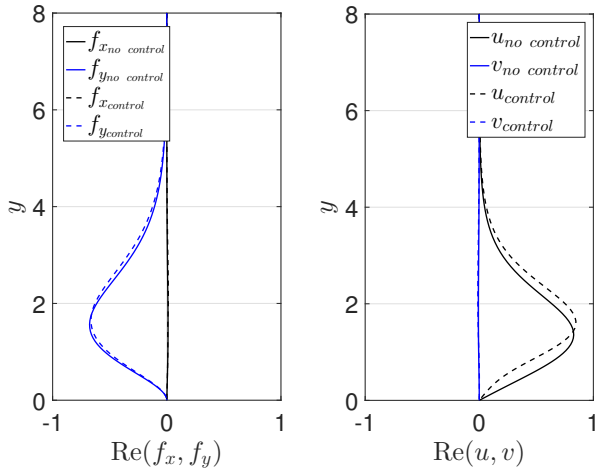

Fig. 6 Real part of forcing and response of the first mode for both controlled and uncontrolled cases (gaussian sensors and actuators placed at $y_a = 1.5$ and $y_s = 0.5$).

and response have peak around $y = 1.5$, close to the optimal region for sensing and acting. Similarly to the previous analysis, in order to damp the strutures more efficiently, the actuator should reach the region where the optimal forcing has a peak, so it could act in the opposite direction. Furthermore, Figure 6 shows that the control does not change substantially the shape of the forcing/response modes, mainly due to the small amplitude of the actuation. Nevertheless, some damping in the streamwise velocity at the near-wall region can be seen for the controlled case. Even with a small amplitude of actuation, drag reduction could still be obtained using this approach. This can also be induced by analysing the influence of this small amplitude control in the gains, as shown in Figure 7. As can be seen, the effect of the control term is mainly in the principal gain (a reduction of approximately 40% in σ_1), with negligible effect on the other modes for this case.

4.2 Shear Sensor and Gaussian Actuator

Using a different choice of sensor, we performed the resolvent analysis (keeping the same shape of actuator, with $|A_c| = 10^{-4}$, $L_a = 0.2$) and several values of y_a, we obtain the results shown in Fig-

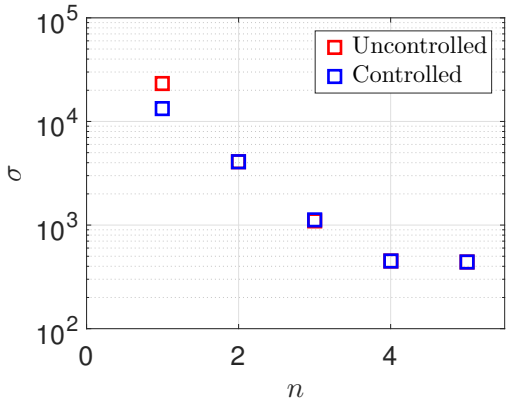

Fig. 7 Gains from the resolvent for both controlled and uncontrolled cases (Gaussian actuators and sensors placed at $y_a = 1.5$ and $y_s = 0.5$).

ure 8, for each component of the forcing. As can be seen, the trend identified in the previous section for the efficiency of each actuation component remains in this case: actuating in the wall-normal and spanwise directions is much more efficient than doing it in the streamwise direction, with the wall-normal being the preferred actuation direction in this case.

This results can also be compared with the previous ones in order to evaluate which kind of sensor is more suitable for this problem. The comparison between the previous sensor and the present one for K_{yu} can be seen in Figure 9, where the center of the Gaussian sensor is set at $y = 0$. It is clear that, for all positions of actuation, the approach with shear sensors is more efficient than the one with velocity sensors, with the results for the shear case reaching reductions up to 10 times larger than the previous case. Moreover, the reduction for shear sensors are present for a wider region of y_a, which can lead to more flexible choice of actuators.

4.3 Shear Sensor and Plasma Actuator

Following the same strategy of the previous analysis, we focus on evaluating the influence of the variation of the stretching parameter h in the first resolvent gain σ_1. The present study differs from the previous one mainly by the length of actuation: now the device is considered to be at the

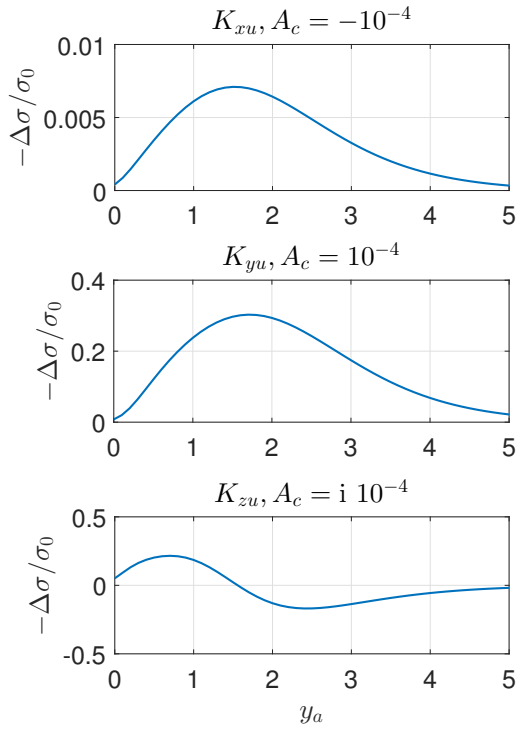

Fig. 8 Sensitivity of the first resolvent gain with change of actuator position for shear sensor at the wall.

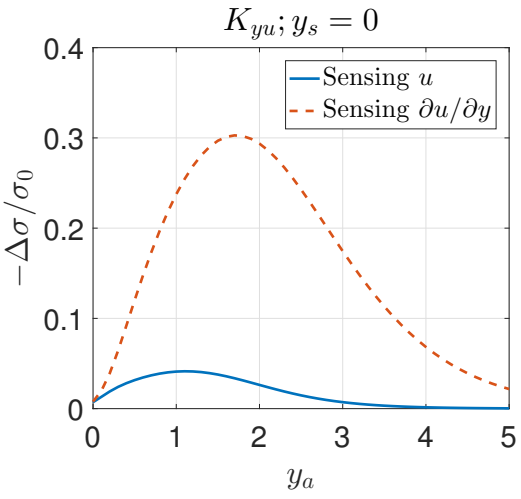

Fig. 9 Comparison of the performance of control between sensing streamwise velocity ($y_s = 0$) or shear at the wall.

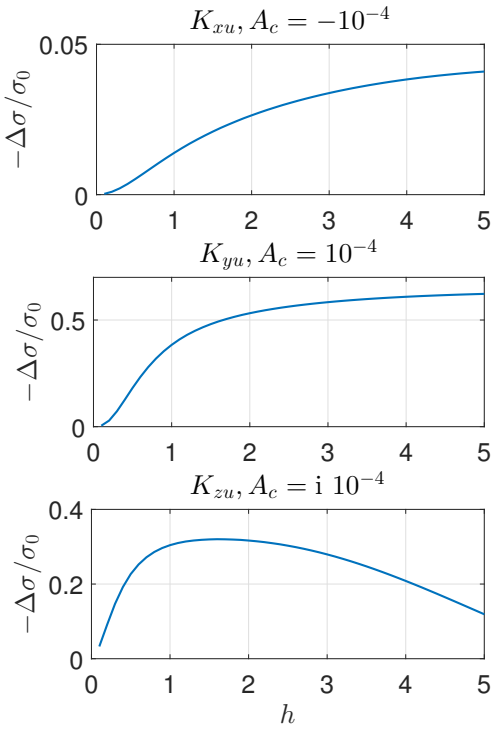

Fig. 10 Variation of first resolvent gain for several values of stretching factor h, considering each of the three components of forcing.

wall with different regions of influence. The results for each component of the control matrix can be seen in Figure 10.

The results show that an actuation without a reasonable spatial support is not as efficient as one extending to upper regions, meaning that a good actuator should reach at least $y = 1$ (with a δ^* normalisation), with better results for higher values of h. This can be explained by the previous analysis: if the actuator has reasonable amplitudes in the regions where the localised actuation is more efficient (for example, in the interval $1 < y < 2.5$, using the information from Figure 9), a higher efficiency will also be obtained for this actuator. If we consider the previous analysis as a numerically approximated impulse response for the actuation, one can see the present case as a convolution between this impulse response and the present shape of actuator, explaining why an actuator with larger spatial support should have better performance. This approach also explains the plateau reached for the K_{xu} and K_{yu} plots: since we are stretching the actuation region, the amplitudes of actuation at the optimal interval mentioned are not reduced substantially, meaning that the reduction of the gains should not change much for increasing values of h. Moreover, since the actuator has a larger spatial support than the Gaussian one, its overall efficiency is also higher. Differently from the other ones, the plot for K_{zu} has a peak and a decay for higher values of h, mainly due to the behaviour identified with the narrow gaussian actuator: since it has a region with positive and negative efficiency (from Figure 9), it is expected that both contributions cancel each other with increase of h.

The influence of this kind of actuation in the gains, response and forcing modes of the resolvent can be seen in Figures 11 and 12 for K_{yu} and $h = 4$. The behaviour follows the trend identified in the first approach, with a reduction of the gains and a change of the peak response, which is moved further away from the wall. The main difference is in the magnitude of reduction (which is approximatelly 60% in σ_1), and in the optimal forcing mode, which presents a new oscilation in the wall-normal direction and a peak in the near wall region for the streamwise forcing. For the optimal response, the results are similar to the ones obtained in the previous analysis, with a decrease of amplitudes in the near wall region, which would potentially delay transition to turbulence due to streaks.

5 Conclusion

We have studied efficient placement of sensors and actuators for closed-loop control of a Blasius boundary layer in a locally parallel framework. For that, we introduce a closed-loop resolvent operator, where the shapes of sensors and actuators are included in a control matrix, which can be changed freely in the formulation.

The Gaussian shape for sensors and actuators was used as a preliminary analysis, since both devices could move to any position in the flow. Still, important conclusions about which component to sense and which direction to act could

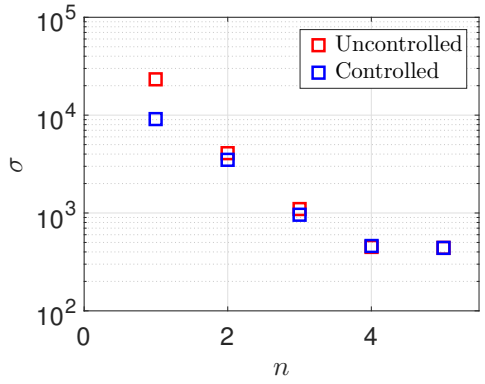

Fig. 11 Gains from the resolvent for both controlled and uncontrolled cases for plasma actuator and shear sensor at the wall ($h = 4$).

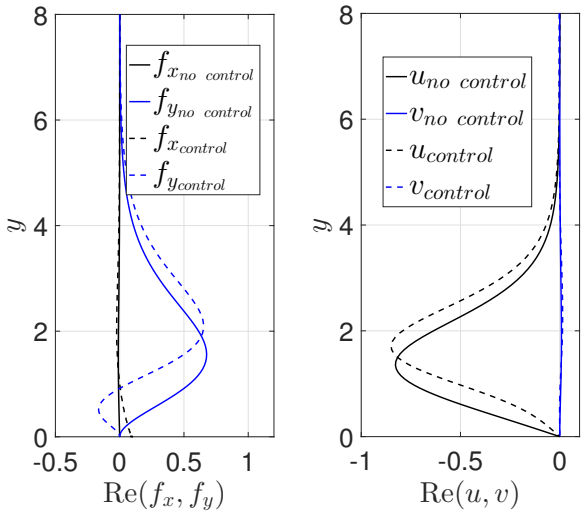

Fig. 12 Forcing and response of the principal mode for both controlled and uncontrolled cases for plasma actuator and shear sensor at the wall ($h = 4$).

be drawn with that approach. Results show that sensing the streamwise component and acting in the wall-normal/spanwise directions is the most efficient way of decreasing the resolvent gains, which would lead to a damping of the most amplified structures in the flow. This conclusion is a consequence of the underlying physics that dominates the studied cases: since we have chosen $k_x = \omega = 0$ and $k_z \neq 0$, the lift-up effect drives the dynamics, where streaks are forced by streamwise vortices.

Going to more realistic configurations, we compared the behaviour of Gaussian sensors and shear sensors, obtaining a considerably higher performance for the latter ones. Finally, we studied the influence of changing the actuator shape, analysing how the spatial support of a given actuator at the wall would change the resolvent gains and the shape of the optimal response. Results show that, as the spatial extent crosses a given threshold in the wall-normal direction, the efficiency does not increase substantially by further increase of that parameter. That result can be useful for actuator design since energetic expense is also a concern in this kind of problem.

Further steps of this work will consider an analytical sensitivity of the resolvent gains with variation of the control matrix, which would give a better idea of best sensor/actuator placement. Furthermore, a method to evaluate the problem in a global resolvent framework, accounting for the divergence of the base flow, is in development, which will lead to conclusions that could be directly applied in experiments.

6 Acknowledgements

This work was done with the support from CISB, the Swedish-Brazilian Research and Innovation Centre, and from Saab AB. Petrônio Nogueira is being funded by a CNPq scholarship.

A The Linearised Navier-Stokes Operators

The operators $\mathbf{A}, \mathbf{B}, \mathbf{C}$ for the locally parallel framework are defined below:

$$\mathbf{A} = \begin{bmatrix} -\mathrm{i}k_x\Delta^{-1}U\Delta + \mathrm{i}k_x\Delta^{-1}U'' + (1/Re)\Delta^{-1}\Delta^2 & 0 \\ -\mathrm{i}k_zU' & -\mathrm{i}k_xU + (1/Re)\Delta \end{bmatrix} \quad (9)$$

$$\mathbf{B} = \begin{bmatrix} \Delta^{-1} & 0 \\ 0 & I \end{bmatrix} \begin{bmatrix} -\mathrm{i}k_x\partial_y & -(k_x^2+k_z^2) & -\mathrm{i}k_z\partial_y \\ \mathrm{i}k_z & 0 & -\mathrm{i}k_x \end{bmatrix} \quad (10)$$

$$\mathbf{C} = \frac{1}{k_x^2+k_z^2} \begin{bmatrix} \mathrm{i}k_x\partial_y & -\mathrm{i}k_z \\ k_x^2+k_z^2 & 0 \\ \mathrm{i}k_z\partial_y & \mathrm{i}k_x \end{bmatrix} \quad (11)$$

where $U' = \frac{\mathrm{d}U}{\mathrm{d}y}(y)$ and $\Delta = \partial_{yy} - k_x^2 - k_z^2$. We keep the non-slip boundary conditions ($\psi = [0\ 0], \partial_y v = 0$ at the boundaries). In summary, the formulation described above can be reduced to the well known Orr-Sommerfeld - Squire system.

References

[1] Ellingsen T and Palm E. Stability of linear flow. *The Physics of Fluids*, Vol. 18, No. 4, pp 487-488, 1975.

[2] Brandt L, Henningson D S and Ponziani D. Weakly nonlinear analysis of boundary layer receptivity to free-stream disturbances. *Physics of Fluids*, Vol. 14, No. 4, pp 1426-1441, 2002.

[3] Brandt L. *European Journal of Mechanics - B/Fluids*, Vol. 47, pp 80-96, 2014.

[4] Schmid P J. Nonmodal stability theory. *Annual Review of Fluid Mechanics*, Vol. 39, pp 129-162, 2007.

[5] Cattafesta III L N and Sheplak M. Actuators for active flow control. *Annual Review of Fluid Mechanics*, Vol. 43, pp 247-272, 2011.

[6] Rowley C W and Dawson S T M. Model reduction for flow analysis and control. *Annual Review of Fluid Mechanics*, Vol. 49, pp 387-417, 2017.

[7] Fabbiane N, Bagheri S and Henningson D S. Energy efficiency and performance limitations of linear adaptive control for transition delay. *Journal of Fluid Mechanics*, Vol. 810, pp 60-81, 2017.

[8] Bagheri S, Brandt L and Henningson D S. Input–output analysis, model reduction and control of the flat-plate boundary layer. *Journal of Fluid Mechanics*, Vol. 620, pp 263-298, 2009.

[9] Hwang Y and Cossu C. Amplification of coherent streaks in the turbulent Couette flow: an input–output analysis at low Reynolds number. *Journal of Fluid Mechanics*, Vol. 643, pp 333-348, 2010.

[10] Jovanovic M R and Bamieh B. Componentwise energy amplification in channel flows. *Journal of Fluid Mechanics*, Vol. 534, pp 145-183, 2005.

[11] Fabbiane N, Simon B, Fischer F, Grundmann S, Bagheri S and Henningson D S. On the role of adaptivity for robust laminar flow control. *Journal of Fluid Mechanics*, Vol. 767, pp R1, 2015.

[12] Kotsonis M, Ghaemi S, Veldhuis L and Scarano F. Measurement of the body force field of plasma actuators. *Journal of Physics D: Applied Physics*, Vol. 44, No. 4, pp 045204, 2011.

Contact Author Email Address

mailto: petronio@ita.br

Copyright Statement